RESEARCH ARTICLE | AUGUST 01 1977

Kinetic theory of tearing instabilities

J. F. Drake; Y. C. Lee

Phys. Fluids 20, 1341–1353 (1977)
https://doi.org/10.1063/1.862017

Kinetic theory of tearing instabilities

J. F. Drake and Y. C. Lee

Department of Physics, University of California, Los Angeles, California 90024
(Received 20 December 1976)

The transition of the tearing instability from the collisional to the collisionless regime is investigated kinetically using a Fokker–Planck collision operator to represent electron-ion collisions. As a function of the collisionality of the plasma, the tearing instability falls into three regions, which are referred to as collisionless, semi-collisional, and collisional. The width Δ of the singular layer around $\mathbf{k}\cdot\mathbf{B}_0 = 0$ is limited by electron thermal motion along $\mathbf{B}_0$ in the collisional and semi-collisional regimes and is typically smaller than ρ_i, the ion Larmor radius. Previously accepted theories, which are based on the assumption $\Delta \gg \rho_i$, are found to be valid only in the collisional regime. The effects of density and temperature gradients on the instabilities are also studied. The tearing instability is only driven by the temperature gradient in the collisional and semi-collisional regimes. Numerical calculations indicate that the semi-collisional tearing instability is particularly relevant to present day high temperature tokamak discharges.

I. INTRODUCTION

Tearing instabilities are believed to be important in a wide variety of physical phenomena ranging from reconnection in the magnetosphere to magnetic oscillations observed in tokamak discharges.[1,2] Consequently there has been a substantial amount of research devoted primarily, until very recently, to the linear stability analysis. Initial investigations[3,4] of the linear tearing instability assumed that the plasma is a resistive medium, and therefore, the electric field $\mathbf{E}$, the magnetic field $\mathbf{B}$, and the plasma current $\mathbf{J}$ are related through Ohm's law,

$$\mathbf{E} + (\mathbf{v}\times\mathbf{B})/c = \eta\mathbf{J}\,, \tag{1}$$

where η is the Spitzer–Härm resistivity.[5] Subsequent authors,[6,7] recognizing that fusion and magnetospheric plasmas were likely to be virtually collision-free, extended the calculation to the collisionless regime by including electron inertia. The inclusion of electron and ion gradient drifts lead to the drift-tearing mode.[8] Recently, Hazeltine *et al.*,[9] unified all these previous calculations by carrying out a kinetic theory including the full electron-electron and electron-ion collision operators. In addition to recovering known results, they found that the tearing mode could be driven unstable by temperature gradients.

Much of the recent interest in the tearing instability has been stimulated by the observation of these modes in recent tokamak discharges.[1,2,10] The tearing modes are believed to have two important effects in tokamaks. First, the magnetic perturbations associated with the modes may lead to a disruption of the magnetic surfaces,[11] resulting in enhanced particle and energy transport. Hazeltine *et al.*,[12] have, for example, shown that the temperature gradient can destabilize the tearing instability. The eventual nonlinear evolution of the instability then relaxes the original gradient, the overall process resulting in an enhanced thermal conductivity. Second, there is some evidence that the tearing mode may play a role in the "disruptive instability".[13] The $m = 2$ tearing mode is typically observed as a precursor to the disruption.

The primary goal of recent nonlinear investigations of the tearing instability in tokamaks is first, to provide estimates of the magnetic field perturbations in the nonlinear state so that the magnitude of the enhanced transport associated with these fluctuations can be evaluated and second, to understand the relationship between the $m = 2$ tearing mode and the disruptive instability. Most of the existing nonlinear theories,[14] however, have been based on the *collisional* magnetohydrodynamic equations. It is not entirely clear that the characterization of present or future tokamak discharges as collisional media is correct even in a qualitative sense. The original motivation behind the present study was to ascertain whether present or future tokamak discharges were in the collisionless regime of the tearing instability and if so, to try to extend the nonlinear theory of the tearing mode to this regime. In carrying out this investigation, however, we found that the previously mentioned linear theories of the collisionless tearing instabilities[7,9] are not correct. In the present manuscript we, therefore, concentrate on the linear aspects of the tearing mode. A subsequent paper will be devoted to the nonlinear aspects of the collisionless and semi-collisional tearing instabilities.

To understand why existing theories of the collisionless tearing instabilities are inadequate, it is convenient to present a qualitative picture of the instability in slab geometry. Referring to Fig. 1, we consider a slab of current J_z of width a, uniform in the y-z plane moving along a large B_z field. A self-consistent $B_y(x)$ ($|B_y| \ll |B_z|$) field is produced which reverses direction across the current sheet [$B_y(0) = 0$].

In the absence of nonideal magnetohydrodynamic effects such as inertia or resistivity, this current sheet is stable since all perturbations in which the plasma remains frozen to the magnetic field lines result in an increase in the magnetic energy of the system. Finite inertia or resistivity, however, allows the tearing instability to relax the system to a lower magnetic energy state. In particular, the tearing mode results in a bunching of the current into filaments along the y direction. An x-y projection of the magnetic topology of this instability along with the directions of the plasma flow (see arrows) are shown in Fig. 2. The B field lines

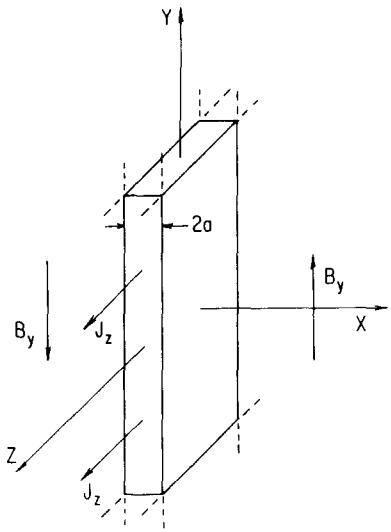

FIG. 1. The equilibrium current distribution is shown in slab geometry. The current J_z runs along an externally produced field B_z, generating a self-consistent $B_y(x)$. We assume $|B_y| \ll |B_z|$.

tear and reconnect near the central layer (around $x \approx 0$ where $\mathbf{k} \cdot \mathbf{B} = 0$) forming the characteristic magnetic islands of the tearing mode. Within the central layer the field lines slip with respect to the plasma, producing an induced electric field $\tilde{E}_z$ which accelerates the electrons along the local magnetic field. The perturbed current $\tilde{J}_z$ which results is localized to a region $x \leq \Delta \ll a$ and, of course, along with the current in the outer region, self consistently generates the magnetic field shown in Fig. 2. In the outer region ($|x| > \Delta$), the field lines remain frozen into the plasma as in the kink mode. In the tearing instability the released magnetic energy in the outer region is converted into the *internal* kinetic energy of the plasma in the central layer (thermal energy in the collisional case and electron kinetic energy in the collisionless case).

The energy flow in the tearing mode should be contrasted with that of the ideal magnetohydrodynamic kink mode, which is unstable in cylindrical geometry. The magnetic energy released in this instability is converted into the kinetic energy of the *macroscopic* plasma motion.

The width Δ of the current layer $\tilde{J}$ produced by the parallel electric field is an important quantity which must be determined from the plasma dynamics in the layer. Previous authors[3,4,7-9] have assumed that $\Delta \gg \rho_i$, where $\rho_i = v_i/\Omega_i$ is the ion Larmor radius, v_i and Ω_i being the ion thermal velocity and cyclotron frequency, respectively. However, an important conclusion of our work is that Δ becomes much smaller than ρ_i as the plasma approaches the collisionless regime (to be defined later). Previous theories are, therefore, not valid in this region. The goal of the present work is to correctly extend the stability analysis to the collisionless regime and to carefully examine the transition from the collisional to the collisionless regimes.

To simplify the mathematical manipulations, we will carry out our calculations in slab geometry. Because $\Delta \ll a$, the dynamics of the layer are relatively insensitive to the geometry under consideration and our slab results can be readily extended to cylindrical geometry.[4,10] The neglect of toroidal effects in tokamak applications is perhaps more difficult to justify.

Our basic procedure is to calculate the electron response by means of a Fokker–Planck equation which only includes the collision operator for electron-ion collisions. This pitch angle scattering model (Lorentz gas) is only rigorously justified in a high Z plasma[5] although our results should be at least qualitatively correct when $Z \sim 1$ or 2. The ions are treated collisionlessly.

Our most important conclusion is that as a function of the collisionality of the plasma, the tearing instability can be separated into three regimes, which we refer to as "collisionless", "semi-collisional," and "collisional".

The growth rate γ of the pure tearing instability (neglecting gradient drifts) is independent of ν_c in the collisionless regime and scales as $\nu_c^{1/3}$ and $\nu_c^{3/5}$ in the semi-collisional and collisional regimes, respectively, where ν_c is the electron-ion collision frequency. The collisionless growth rate γ_k, which differs from that in Refs. 7 and 9, has been previously obtained by Laval *et al.*,[15] while our collisional results are in agreement with previous calculations.[3,4] The semi-collisional region was previously unknown and appears to be particularly relevant to present tokamak discharges.

When we include temperature and density gradient drifts, previously known instabilities,[8] including the temperature gradient driven mode of Hazeltine *et al.*,[9] are obtained. The collisionless and semi-collisional versions of these modes are also presented.

In Sec. II, we illustrate the basic physical mechanisms which govern the dynamics of the pure tearing mode by presenting a heuristic derivation of the three regimes of this instability. This presentation also serves to motivate the more rigorous but detailed calculations which

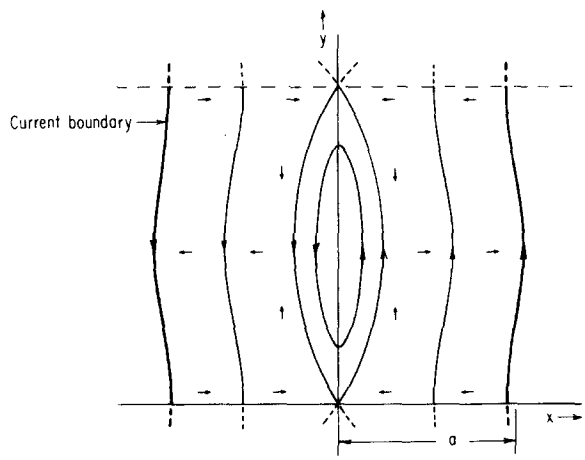

FIG. 2. The magnetic topology of the tearing instability is shown. The current slab of Fig. 1 has been subjected to a tearing instability with $k_z = 0$. $\mathbf{k} \cdot \mathbf{B}_0 = k_y B_{0y} = 0$ at $x = 0$. The short arrows indicate the direction of plasma flow.

follow. The equilibrium and general equations are presented in Sec. III. In Secs. IV and V we first investigate the collisionless and then the semi-collisional and collisional tearing instability. Section VI is devoted to a discussion of the results of our calculations.

II. HEURISTIC DERIVATION OF THE TEARING INSTABILITY

We investigate the stability of the current slab previously discussed in Fig. 1 to a perturbation with wavenumber k_y and growth rate γ of the form shown in Fig. 2. The magnetic perturbations can be represented by a vector potential $\tilde{A}_z$ as follows:

$$\tilde{B}_x = ik_y \tilde{A}_z(x, y, t) \; ; \tag{2a}$$

$$\tilde{B}_y = -\partial \tilde{A}_z / \partial x \; . \tag{2b}$$

An induced electric field

$$\tilde{E}_z = -\gamma \tilde{A}_z / c \tag{3}$$

is generated which has a component $\tilde{E}_\parallel = \tilde{E}_z \cos\theta(x)$ along B_0 (see Fig. 3). A large electron current $\tilde{J}_\parallel$ will result from this field unless one of the following two physical effects occurs:

(1) The Doppler frequency ω_D resulting from electron thermal motion along $\mathbf{B}_0$ is greater than γ

$$\omega_D \gg \gamma \; , \tag{4}$$

causing the electrons to feel an ac rather than a dc acceleration and thus reducing the response $\tilde{J}_\parallel$. When $\gamma \gg \nu_c$, the electrons stream along $\mathbf{B}_0$ at their thermal velocity v_e and $\omega_D = k_\parallel v_e$. In the opposite limit, $\gamma \ll \nu_c$, collisions inhibit electron motion along $\mathbf{B}_0$ and the electrons diffuse along the field lines with a diffusion coefficient $D = v_e^2/\nu_c$. The resulting effective Doppler frequency of the electrons is $\omega_D = k_\parallel^2 D$.

(2) An electrostatic field $\tilde{E} = -\nabla\tilde{\phi}$ is produced which cancels the parallel component of the induced field (see Fig. 3)

$$\tilde{E}_\parallel = -\cos\theta \gamma \tilde{A}_z / c - ik_\parallel \tilde{\phi} \approx 0 \; . \tag{5}$$

Figure 4 illustrates the mechanism by which ϕ is generated [$\theta(x) \ll 1$ is enlarged for clarity]. The induced electric field causes the electrons to move with velocity

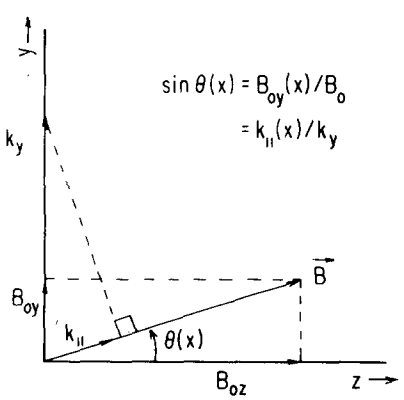

FIG. 3. The vector directions of k and $\mathbf{B}_0$ are shown. Near $x = 0$, $k_\parallel = k_y x/l_s$, where $l_s = B_0/(\partial B_{0y}/\partial x)$.

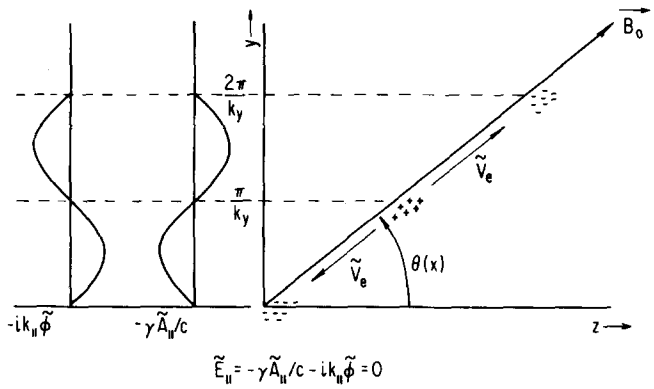

FIG. 4. The physical mechanism responsible for the generation of ϕ is illustrated. The parallel induced field $-\gamma\tilde{A}_\parallel/c$ causes the electrons to flow with velocity $\tilde{v}_e$ as shown. The resulting charge separation produces a parallel electrostatic field $-ik_\parallel\tilde{\phi}$ which tends to cancel the parallel induced field. For sufficiently large $k_\parallel$, $\tilde{E}_\parallel \to 0$, i.e., the electrons "short out" the parallel induced field.

$\tilde{v}_e$ as shown, causing a reduction in the electron density around $y = \pi/k_y$, and an increase around 0 and $2\pi/k_y$. The potential which results tends to cancel the induced field. The magnitude of $\tilde{\phi}$ evidently increases with $k_\parallel$ since $\tilde{\phi} = 0$ where $k_\parallel = 0$. When $k_\parallel$ is sufficiently large, the electron motion along B_0 effectively "shorts out" the parallel component of the induced field.

We conclude therefore that unless $k_\parallel \simeq 0$, either (4) or (5) is satisfied and $\tilde{J}_\parallel$ is small. Since $k_\parallel = 0$ at $x = 0$ and varies as

$$k_\parallel = k_y x / l_s \tag{6}$$

around this point, l_s being the magnetic shear length, the induced current $\tilde{J}_\parallel$ is localized to a region $|x| < \Delta \ll a$. This narrow current layer produces a discontinuity in $\tilde{B}_y$, which we roughly evaluate by integrating the z component of Maxwell's equation as follows:

$$[\tilde{B}_y(x)]_{-\Delta}^{\Delta} \approx (4\pi/c)\,\Delta \tilde{J}_z(x = 0) \; . \tag{7}$$

Since $\tilde{J}_z \propto \tilde{A}_z$, we conveniently eliminate $\tilde{B}_y$ using (2b), thus,

$$[\partial \tilde{A}_z(x)/\partial x]_{-\Delta}^{\Delta} \simeq -(4\pi/c)\tilde{J}_z \Delta \; . \tag{8}$$

The slope of $\tilde{A}_z$ is therefore discontinuous across the region of particle acceleration. Note, however, that although $\partial\tilde{A}_z/\partial x$ is discontinuous, implicit in the approximation leading to (7) is the assumption that $\tilde{A}_z \simeq$ const across the layer, i.e., the width Δ arises as a result of one of the two effects discussed in (4) and (5) and not because of the variation of $\tilde{A}_z$.

The discontinuity in $\partial\tilde{A}_z/\partial x$ across the layer must, of course, match a corresponding discontinuity in the solutions for $\partial\tilde{A}_z/\partial x$ in the outer region. Since $\tilde{E}_\parallel = 0$ in this region, the ideal magnetohydrodynamic equations are valid and the solutions to the equation for $\tilde{A}_z$ are well known.[4,11] For convenience, the discontinuity in the outer solutions is simply represented by

$$\Delta' = (\partial \tilde{A}_z/\partial x)_{-\Delta}^{\Delta} / \tilde{A}_z(0) \; . \tag{9}$$

The explicit value of Δ' varies with the geometry of

interest (cylidrical,[11] slab,[4] or toroidal) and with the particular current distribution J_0 under consideration. Generally, however, Δ' scales as a^{-1}, which is consistent with $\tilde{A}_z(x)$ having a scale length of order a. Treating Δ' as a known function, we can then rewrite (8) as

$$\Delta'\tilde{A}_z = -(4\pi/c)\Delta\tilde{J}_z(0). \tag{10}$$

The dispersion relation then follows immediately once $\tilde{J}_z$ and Δ are evaluated. Note also that since Δ' depends only on the plasma parameters in the outer region, the total current in the central layer, represented roughly by $\tilde{J}_z(0)\Delta$, is independent of the detailed structure of the layer.

We consider the three previously mentioned regimes independently.

A. Collisionless regime

The plasma can be considered collisionless if

$$\gamma \gg \nu_c . \tag{11}$$

The electron drift velocity in response to the electric field given in (3) is then

$$\tilde{v}_{ez} = e\tilde{A}_z/mc , \tag{12}$$

where m is the electron mass. The resultant current becomes

$$\tilde{J}_z = -n_{0e}e^2\tilde{A}_z/mc , \tag{13}$$

n_{0e} being the local equilibrium electron number density. $\omega_d = k_\parallel v_e \gg \gamma$ before $E_\parallel \to 0$ so the region of particle acceleration is defined by

$$k_\parallel v_e = k_y v_e \Delta/l_s = \gamma , \tag{14}$$

or

$$\Delta = \gamma l_s/k_y v_e . \tag{15}$$

Combining (10), (13), and (15), we obtain the growth rate[15]

$$\gamma_k \simeq (\Delta' k_y a^2)(v_e/l_s)(k_0 a)^{-2} \approx (v_e/l_s)(k_0 a)^{-2} , \tag{16}$$

where $k_0^{-1} = c/\omega_{pe}$ is the collisionless skin depth and $\omega_{pe} = (4\pi n_{0e}e^2/m)^{1/2}$ is the local electron plasma frequency. The width of the layer then follows from (15)

$$\Delta_k = (\Delta' a)/k_0^2 a \approx (k_0^2 a)^{-1} . \tag{17}$$

Typically, $k_0 a \gg 1$ so $\Delta_k \ll k_0^{-1}$. Moreover, in most fusion discharges $k_0\rho_i > 1$, which implies $\Delta_k \ll \rho_i$. Previous collisionless theories[7,9] which were based on the assumption that $\Delta_k \gg \rho_i$ are clearly invalid. The results in (16) and (17) are only correct, of course, if the inequality in (11) is satisfied.

B. Semi-collisional regime

If $\gamma < \nu_c$, electron collisions with ions limit the electron response to the parallel electric field and

$$\tilde{J}_z = \tilde{E}_z/\eta = -\gamma\tilde{A}_z/c\eta . \tag{18}$$

In the semi-collisional regime, as in the collisionless regime, $\omega_d \gg \gamma$ before $E_\parallel \to 0$ so Δ is defined by

$$k_\parallel^2 v_e^2/\nu_c = k_y^2\Delta^2 v_e^2/\nu_c l_s^2 = \gamma \tag{19}$$

or

$$\Delta = (\nu_c\gamma)^{1/2} l_s/k_y v_e . \tag{20}$$

The growth rate then follows from (10), (18), and (20)[16]

$$\gamma \simeq \gamma_k^{2/3}\nu_c^{1/3} . \tag{21}$$

From (20), the width of the current layer is

$$\Delta = (\nu_c/\gamma_k)^{2/3}\Delta_k . \tag{22}$$

As ν_c becomes larger than γ_k the region of particle acceleration broadens from the collisionless width. Collisions with ions reduce the effective electron velocity along the magnetic field, allowing more particles to receive a dc acceleration, thus broadening the layer.

It should be emphasized that the ions essentially play no role in the collisionless and semi-collisional tearing modes because the electron response to $\tilde{E}_\parallel$ is much larger than that of the ions. The ion motion is important, however, in the collisional tearing mode where electrostatic effects must be included.

C. Collisional regime

If the electron-ion collision frequency is very large, the electrons are strongly inhibited from flowing along the magnetic field lines. The effective Doppler frequency experienced by the electrons is thereby strongly reduced. Under these conditions $\tilde{E}_\parallel$ "shorts out" before $\omega_d > \gamma$. We must therefore include electrostatic effects in our analysis.

The electron response to $\tilde{E}_\parallel$ is limited by collisions so from the momentum equation

$$\tilde{v}_{e\parallel} = -e\tilde{E}_\parallel/m\nu_c = -e(-\gamma\tilde{A}_z/c - ik_\parallel\tilde{\phi})/m\nu_c , \tag{23}$$

The electron density perturbation $\tilde{n}_e$ resulting from this parallel motion then follows from the linearized continuity equation

$$\tilde{n}_e = -ik_\parallel\tilde{v}_{e\parallel}n_{0e}/\gamma = ik_\parallel e n_{0e}\tilde{E}_\parallel/m\nu_c\gamma . \tag{24}$$

The electron gyrofrequency $\Omega_e \gg \gamma$ so the density perturbation arising from the perpendicular motion is negligible.

The ion response to the fields depends strongly on the relationship between Δ and ρ_i. In the collisional regime we assume $\Delta \gg \rho_i$, so the ions can be considered magnetized. This assumption must, of course, be verified after Δ is calculated self-consistently. The ion polarization drift produces a density perturbation $\tilde{n}_i$ given by

$$\tilde{n}_i = (c^2/4\pi Zec_A^2)\partial^2\tilde{\phi}/\partial x^2 , \tag{25}$$

where we have assumed $\partial/\partial x \gg k_y$, $c_A = (B_0^2/4\pi n_{0i}M)^{1/2}$ is the Alfvén velocity, and $n_{0i} = n_{0e}/Z$, M and Z are the equilibrium ion number density, mass, and charge, respectively. Demanding charge neutrality,

$$\partial^2\tilde{\phi}/\partial x^2 = ik_\parallel(\Omega_e\Omega_i/\gamma\nu_c)\tilde{E}_\parallel = ik_\parallel(\Omega_e\Omega_i/\gamma\nu_c)(-\gamma\tilde{A}_z/c - ik_\parallel\tilde{\phi}) . \tag{26}$$

The induced electric field in (26) clearly leads to the generation of an electrostatic field when $k_\parallel \neq 0$ as discussed in Fig. 4. When $k_\parallel$ is small, $\partial^2\tilde{\phi}/\partial x^2 \gg k_\parallel^2(\Omega_e\Omega_i/\gamma\nu_c)\tilde{\phi}$ and $\tilde{\phi}$ is negligible, but when the inequality is re-

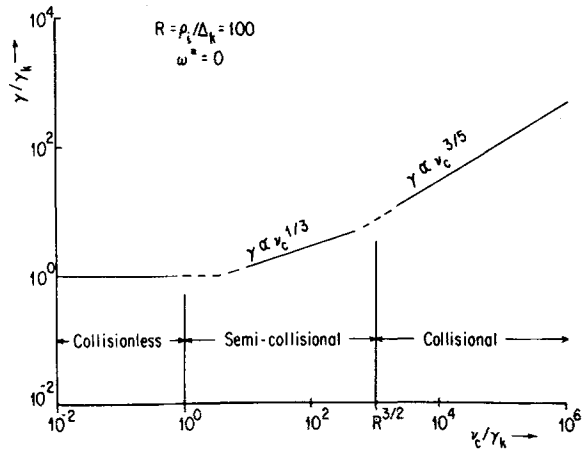

FIG. 5. The growth rate γ of the tearing mode ($\omega^* \approx 0$) is shown as a function of the electron-ion collision frequency ν_c. Both γ and ν_c are normalized to γ_k the collisionless growth rate (see Table I). The dependence of γ on ν_c is indicated on each of the three regions.

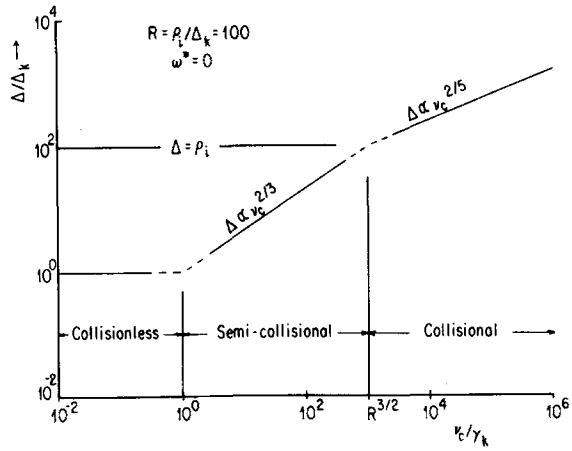

FIG. 6. The width Δ of the region of particle acceleration ("singular layer") is shown as a function of ν_c. Δ has been normalized to the collisionless width $\Delta_k \approx (k_0^2 a)^{-1} \ll k_0^{-1}$, where k_0^{-1} is the collisionless skin depth (see Table I). Note that the boundary between collisional and semi-collisional regimes occurs where $\Delta \simeq \rho_i$.

versed for large $k_\parallel$, $\tilde{E}_\parallel \simeq 0$. The point where $\tilde{E}_\parallel \to 0$, which defines Δ, occurs when

$$\partial^2\tilde{\phi}/\partial x^2 \approx \tilde{\phi}/\Delta^2 \approx (\Omega_e \Omega_i/\gamma\nu_c)(k_y\Delta/l_s)^2\tilde{\phi} \tag{27}$$

or

$$\Delta \approx (\Omega_e \Omega_i/\gamma\nu_c)^{-1/4}(l_s/k_y)^{1/2} . \tag{28}$$

The parallel electron current at $x = 0$ is still given by (18), which, in conjunction with (10) and (28), yield the classic growth rate of the collisional tearing mode[4]

$$\gamma_c \simeq \nu_c^{3/5}\gamma_k^{2/5}(\Delta_k/\rho_i)^{2/5} \propto \nu_c^{3/5}B^{2/5} . \tag{29}$$

The width of the current layer is, from (28),

$$\Delta_c \simeq (\nu_c/\gamma_k)^{2/5}\rho_i^{2/5}\Delta_k^{3/5} , \tag{30}$$

which must be greater than ρ_i so the collisional tearing mode analysis is valid when

$$\nu_c/\gamma_k > (\rho_i/\Delta_k)^{3/2} . \tag{31}$$

The previous semi-collisional tearing mode calculation is correct as long as the current channel width in (22) resulting from the Doppler frequency of the electrons is smaller than that in (30) which is based on $\tilde{E}_\parallel \to 0$. This condition merely reproduces (31) with the inequality reversed. Consequently, the boundary between the collisional and semi-collisional tearing modes occurs at $\nu_c/\gamma_k \simeq (\rho_i/\Delta_k)^{3/2}$. A comparison of the growth rates in (21) and (30) shows that γ is approximately continuous across this region.

The transition of the tearing mode from the collisionless to the collisional regime is illustrated in Figs. 5 and 6 where γ and Δ are shown as functions of ν_c. The dashed portions of the curves indicate the transition regions where our results are not accurate. Both γ and Δ increase monotonically with ν_c. Δ increases from a width less than k_0^{-1} in the collisionless regime to ρ_i at the boundary between the semi-collisional and collisional regimes. The analytic expressions for γ and Δ in the three regions are summarized in Table I. The relevance of these results to tokamak discharges is discussed in Sec. VI.

III. GENERAL EQUATIONS

We now investigate the tearing instability in a more rigorous and systematic manner, including both tem-

TABLE I. Tearing instability.

	$\omega^* = 0$		
	Growth rate	Width of layer	Restrictions
I Collisionless	$\gamma_k = \dfrac{k_y v_e(\Delta' a)}{2\pi^{1/2}k_0^2 a l_s}$	$\Delta_k = \dfrac{\Delta' a}{2\pi^{1/2}k_0^2 a}$	$\nu_c \ll \gamma_k$
II Semi-collisional	$\gamma = \left(\dfrac{3\pi^{1/4}}{4\Gamma(11/4)}\right)^{2/3}\gamma_k^{2/3}\nu_c^{1/3}$	$\Delta \simeq (\nu_c/\gamma_k)^{2/3}\Delta_k$	$1 \ll \nu_c/\gamma_k \ll (\rho_i/\Delta_k)^{3/2}$
III Collisional	$\gamma_c = \left(\dfrac{\Gamma(1/4)}{2\pi\Gamma(3/4)}\right)^{4/5}(k_y a^2/l_s)^{2/5} \times (\Delta' a)^{4/5}\tau_A^{-2/5}\tau_s^{-3/5}$ $= \dfrac{1}{8}\left(\dfrac{27\pi T_i}{ZT_e}\right)^{1/5}\left(\dfrac{\Gamma(1/4)}{\Gamma(3/4)}\right)^{4/5} \times \nu_c^{3/5}\gamma_k^{2/5}(\Delta_k/\rho_i)^{2/5}$	$\Delta_c \simeq (\nu_c/\gamma_k)^{2/5}\rho_i^{2/5}\Delta_k^{3/5}$	$\nu_c/\gamma_k \gg (\rho_i/\Delta_k)^{3/2}$

perature and density gradient drifts. The initial equilibrium is basically that previously discussed in Fig. 1. The density, current, and temperature vary only in the x direction and B_{0y} reverses sign at $x=0$. For simplicity, we neglect the effect of collisions on the equilibrium plasma configuration and the associated electric field required to maintain J_0. Under the assumption that the plasma pressure is balanced by magnetic forces, electrostatic equilibrium fields can also be neglected. The equilibrium plasma distributions $f_{0\alpha}(\mathbf{x}, \mathbf{v})$, for particles of species α, can then be simply expressed as functions of the constants of motion, which consist of the particle energy,

$$H = m_\alpha v^2/2 \tag{32a}$$

and the y and z canonical momenta, P_y and P_z, respectively, where

$$\mathbf{P} = m_\alpha \mathbf{v} + q_\alpha \mathbf{A}_0/c \tag{32b}$$

and $\mathbf{A}_0(x)$ is the equilibrium vector potential. The plasma currents resulting from the specification of $f_{0\alpha}(H, P_y, P_z)$ must, of course, be self-consistent with the density and temperature gradients and the magnetic field $\mathbf{B}_0 = \nabla \times \mathbf{A}_0$. For example, near $x=0$ we represent f_0 as

$$f_0(H, P_y, P_z) = f_M[1 + P_z U_z/T + P_y U_y^n/T + P_y U_y^T(H - 3T/2)/T^2] , \tag{33a}$$

where

$$f_M = \exp(-H/T)/\pi^{3/2} v_\alpha^3 ; \tag{33b}$$

$$U_y^n = cT(\partial n_0/\partial x)/qB_0 n_0 ; \tag{33c}$$

$$U_y^T = c(\partial T/\partial x)/qB_0 ; \tag{33d}$$

$$U_{ze} = -cB_0/4\pi n_{0e} e l_s ; \tag{33e}$$

$$U_{zi} = 0 . \tag{33f}$$

U_y^n and U_y^T are the diamagnetic drift velocities associated with the density and temperature gradients, respectively. The species index α has been supressed in (33a) to (33d) for simplicity. Charge neutrality requires $U_{ye}^n/T_e = -ZU_{yi}^n/T_i$. The parallel electron drift U_{ze} is assumed to be large compared with that of the ions but small compared with v_e.

We consider the response of this equilibrium to a pertrubation of wave vector k_y and complex frequency ω as shown in Fig. 2. Such a perturbation is completely general as long as the density and temperature gradients near $x=0$ are arbitrary. The perturbed fields are represented by a vector potential $\tilde{\mathbf{A}}(x, y, t)$ and a scalar potential $\tilde{\phi}(x, y, t)$ as

$$\tilde{\mathbf{B}} = \nabla \times \tilde{\mathbf{A}} ; \tag{34a}$$

$$\tilde{\mathbf{E}} = i\omega\tilde{\mathbf{A}}/c - \nabla\tilde{\phi} . \tag{34b}$$

$\tilde{\mathbf{A}}$ is driven by the perturbed plasma currents

$$\nabla^2\tilde{\mathbf{A}} = -(4\pi/c)(\tilde{\mathbf{J}}_e + \tilde{\mathbf{J}}_i) \tag{35}$$

with $\tilde{\phi}$ being produced by the associated density perturbations

$$\nabla^2\tilde{\phi} = 4\pi e(\tilde{n}_e - Z\tilde{n}_i) . \tag{36}$$

As in Sec. II, we are primarily concerned with the plasma response in the central layer. In this region a number of simplifying assumptions can be made:

(1) The current $\tilde{\mathbf{J}}$ which is produced by the induced electric field is primarily along the z direction (direction of $\mathbf{B}_0$) so $\tilde{\mathbf{A}}$ in (35) is dominated by its z component and $\tilde{A}_x$ and $\tilde{A}_y$ can be neglected.

(2) The parallel response of the electrons to the induced field is much larger than that of the ions so $\tilde{J}_{ze} \gg \tilde{J}_{iz} \simeq 0$.

(3) $\partial^2/\partial x^2 \gg k_y^2 \simeq a^{-2}$.

Equations (35) and (36) then simplify to

$$\partial^2\tilde{A}_z/\partial x^2 = -(4\pi/c)\tilde{J}_{ze} ; \tag{37}$$

$$\partial^2\tilde{\phi}/\partial x^2 = 4\pi e(\tilde{n}_e - Z\tilde{n}_i) . \tag{38}$$

The first order electron distribution is assumed to satisfy a Fokker–Planck equation containing only electron-ion collisions[17]:

$$[\partial/\partial t + \mathbf{v}\cdot\partial/\partial\mathbf{x} - \Omega_e\partial/\partial\phi - (\nu/2)(\partial/\partial\mathbf{v})\cdot(v^2\mathbf{I} - \mathbf{vv})\cdot(\partial/\partial\mathbf{v})]\tilde{f}_e = (e/m)[\tilde{\mathbf{E}} + (\mathbf{v}\times\tilde{\mathbf{B}})/c]\cdot(\partial/\partial\mathbf{v})f_{0e} = e[\tilde{\mathbf{E}} + (\mathbf{v}\times\tilde{\mathbf{B}})/c]\cdot[\mathbf{v}\partial/\partial H + \partial/\partial\mathbf{P}]f_{0e} \tag{39}$$

where

$$\nu(v) = 4\pi n_{0i} Z^2 e^4 \ln\Lambda/m^2 v^3 ,$$

$\ln\Lambda$ is the Coulomb logarithm and ϕ is the poloidal angle of a cylindrical velocity coordinate system with its axis along $\mathbf{B}_0$. In writing (39), we have invoked assumption (2) to neglect the ion drift velocity. When $\omega \ll \Omega_e$ and $\Delta \gg \rho_e$, $\rho_e = v_e/\Omega_e$ being the electron Larmor radius, the ϕ dependence of $\tilde{f}_e$ is weak and we can average (39) over this angle. After using (34) and re-arranging terms, we find

$$[i(\omega - k_\parallel v_\parallel) + (\nu/2)(\partial/\partial\xi)(1-\xi^2)(\partial/\partial\xi)][\tilde{f}_e - (e\tilde{A}_z/c)\partial f_{0e}/\partial P_z] = -e\tilde{E}_\parallel v_\parallel \partial f_{0e}/\partial H + e(\tilde{\phi} - \tilde{A}_\parallel v_\parallel/c)ik_y\partial f_{0e}/\partial P_y , \tag{40}$$

where the subscript $\parallel$ refers to the component of the vector along $\mathbf{B}_0$ and $\xi = v_\parallel/v$. The term $(e\tilde{A}_z/c)\partial f_{0e}/\partial P_z$ in (40) is important in the outer region where it represents the current perturbation resulting from a displacement of J_0 in the x direction (see Fig. 2). In the central layer, however, it can be neglected compared with the terms on the right side of (40),[4] yielding the simplified equation,

$$[i(\omega - k_\parallel v_\parallel) + (\nu/2)(\partial/\partial\xi)(1-\xi^2)(\partial/\partial\xi)]\tilde{f}_e = -e\tilde{E}_\parallel v_\parallel(\partial f_{0e}/\partial H) + e(\tilde{\phi} - \tilde{A}_\parallel v_\parallel/c)ik_y\partial f_{0e}/\partial P_y . \tag{41}$$

The first term on the right side of (41) simply describes the electron response to the parallel electric field while the second term contains the perturbations arising from the $\tilde{E}_y/B_{0z}$ drifts in the x direction.

Equations (37), (38), and (41) form the basis of our analyses of the tearing instability. We solve (41) for $\tilde{f}_e$ in the limits $|\omega| \gtrless \nu_c$ and thereafter calculate $\tilde{J}_{ze}$ and $\tilde{n}_e$. The ions are assumed to be magnetized or unmagnetized when $\Delta \gtrless \rho_i$, respectively. The ion density pertrubation $\tilde{n}_i$ then follows after a straightforward linearization of the collisionless Vlasov equation. The coupled, second-order equations [(37) and (38)] for $\tilde{\phi}$ and $\tilde{A}_z$ are solved in appropriate limits to obtain the discontinuity in $\partial\tilde{A}_z/\partial x$ across the layer. This discontinuity, which is again represented by Δ' [see (9)], is known from previous calculations[4,11] so the dispersion relation follows immediately.

IV. COLLISIONLESS TEARING INSTABILITY

In the collisionless tearing instability $|\omega| \gg \nu_c$ and the collision operator in (41) can be neglected, allowing us to solve for $\tilde{f}_e$ directly

$$\tilde{f}_e = ie\tilde{E}_\parallel v_\parallel (\partial f_{0e}/\partial H)/(\omega - k_\parallel v_\parallel) + e(\tilde{\phi} - \tilde{A}_\parallel v_\parallel/c)k_y(\partial f_{0e}/\partial P_y)/(\omega - k_\parallel v_\parallel) . \quad (42)$$

From (33a),

$$\partial f_{0e}/\partial H \simeq - f_{0e}/T_e ; \quad (43a)$$

$$\partial f_{0e}/\partial P_y \simeq [U^n_{ye} + U^T_{ye}(H_e - 3T_e/2)/T_e] f_{0e}/T_e . \quad (43b)$$

The electron current resulting from this perturbed distribution is given by

$$\tilde{J}_{ze} \simeq \tilde{J}_{\parallel e} = - n_{0e} e \int d\mathbf{v}\, v_\parallel \tilde{f}_e . \quad (44)$$

After some algebra, we find

$$J_{ze} \simeq (i\omega^2_{pe}\tilde{E}_\parallel/4\pi\omega)\{[(\omega - \omega^*_n)/\omega]\, s^2 Z'(s) - (\omega^*_T/\omega)Q(s)\} , \quad (45)$$

where

$$\omega^*_n = k_y U^n_{ye} ; \quad (46a)$$

$$\omega^*_T = k_y U^T_{ye} \quad (46b)$$

are the diamagnetic drift frequencies, $Z'(s) \equiv dZ/ds$, where Z is the plasma dispersion function[18] of argument $s = \omega/k_\parallel v_e$, and

$$Q(s) = (2s/\pi^{1/2}) \int_{-\infty}^{\infty} dP(P^2 - 1/2)P^2 \exp(-P^2)/(s - P) = - s^3 Z''(s)/2 . \quad (47)$$

The first order density perturbation follows in a similar way,

$$\tilde{n}_e = n_0 \int d\mathbf{v}\, \tilde{f}_e \simeq - k_\parallel \tilde{J}_{ze}/\omega e + (k^2_{De}\omega^*_n/4\pi\omega e)\tilde{\phi} , \quad (48)$$

where $k_{De} = (2)^{1/2}\omega_{pe}/v_e$ is the electron Debye wavenumber.

In our discussion of the collisionless tearing mode in Sec. II, we found that $\Delta \ll \rho_i$ so the ions respond to $\tilde{\phi}$ as if they were unmagnetized. For the low frequencies associated with the tearing instabilities, the static ion response is appropriate

$$\tilde{n}_i = - k^2_{Di}\tilde{\phi}/4\pi Ze . \quad (49)$$

Combining (48) and (49) with (38) we find that charge separation can be neglected as long as $k_{Di}\Delta \gg 1$ and

$$\tilde{\phi}(k^2_{Di} + k^2_{De}\omega^*_n/\omega) \simeq - k_\parallel(\omega^2_{pe}/\omega^2)(\omega\tilde{A}_z/c - k_\parallel\tilde{\phi}) \times \{[(\omega - \omega^*_n)/\omega]\, s^2 Z'(s) - (\omega^*_T/\omega)Q(s)\} . \quad (50)$$

$\tilde{E}_\parallel$ on the right side of (50) has been written implicitly in terms of $\tilde{A}_z$ and $\tilde{\phi}$. We could immediately solve (50) for $\tilde{\phi}$ and insert this result into (45), leaving, in conjunction with (37), a second-order equation for $\tilde{A}_z$. However, for parameters of interest, we will now show that $\tilde{\phi}$ can be neglected.

The functions $s^2Z'(s)$ and $Q(s)$ are strongly peaked around $k_\parallel = k_y x/l_s = 0$ where $s \to \infty$, the half-widths of both functions occurring where $s \simeq 1$ or $k_\parallel v_e \simeq \omega$. As discussed in Sec. II, when $s = \omega/k_\parallel v_e \ll 1$, the large Doppler frequency felt by an electron reduces its response to the electric field. As long as $|k_\parallel \phi| \ll |\omega\tilde{A}_z/c|$ when $s \gtrsim 1$, $\tilde{\phi}$ can be neglected. This inequality is satisfied when the term proportional to $\tilde{\phi}$ on the left side of (50) is large compared with that on the right side. $\tilde{\phi}$ on the right side of (50) is negligible for $s \gtrsim 1$ if T_i is not too much greater than T_e. In most cases of interest $\tilde{\phi}$ in (45) can then be discarded, leaving the equation

$$\partial^2\tilde{A}_z/\partial x^2 = k^2_0\tilde{A}_z\{[(\omega - \omega^*_n)/\omega]\, s^2 Z'(s) - (\omega^*_T/\omega)Q(s)\} . \quad (51)$$

The discontinuity in the slope of $\tilde{A}_z$ across the current layer can be evaluated by integrating (51) under the assumption that $\tilde{A}_z$ is approximately constant across the layer (constant ψ approximation[4]). Representing the discontinuity by Δ' as defined in (9), the frequency ω^*_1 and growth rate γ_k of the collisionless tearing mode are

$$\omega^*_1 = \omega^*_n + \omega^*_T/2 ; \quad (52a)$$

$$\gamma_k = \mathrm{Im}\,\omega = k_y v_e(\Delta' a)/2k^2_0 a l_s \pi^{1/2} .$$

The growth rate γ_k in (52) differs only slightly from the value obtained in our previous rough calculation. The density and temperature gradients impart a real frequency to the collisionless tearing mode but do not influence the growth rate. This should be contrasted with the collisional regime where both the density and temperature gradients modify the growth of the instability.[8,9]

The width of the current channel is again given by $\Delta \simeq l_s|\omega|/k_y v_e$, or from (52a)

$$\Delta = (1 + \omega^{*2}_1/\gamma^2_k)^{1/2}\Delta_k , \quad (52b)$$

$$\Delta_k = (\Delta' a)/2\pi^{1/2}k^2_0 a . \quad (52c)$$

The gradient drifts broaden the current layer beyond that of the pure tearing mode. Simply stated, as $|\omega| \simeq \omega^*_1$ increases, the Doppler frequency $k_\parallel v_e \propto \Delta$ must be larger before the electron response to the induced field is reduced. However, although Δ increases with ω^*_1, $\tilde{J}_{ze}(0)$ decreases [see (45)] so that the total current in the layer $\simeq \tilde{J}_{ze}\Delta$ remains constant [see (10) and discussion following]. Coppi[8] has previously noted that the gradient drifts broaden the region of particle acceleration in the collisional limit.

The assumption that $\tilde{A}_z$ is constant within the layer requires that the integrated phase across the layer be small. Near $x = 0$, we have from (51) $\partial^2/\partial x^2 \simeq k^2_0(\omega - \omega^*_1)/\omega$ so we require

$$k^2_0\Delta^2|(\omega - \omega^*_1)/\omega| \ll 1 ,$$

or

$$k^2_0\Delta^2_k \ll (1 + \omega^{*2}_1/\gamma^2_k)^{-1/2} . \quad (53)$$

Our present approximations also require $\Delta \ll \rho_i$, although it is shown in Sec. V that (52) is correct even when this restriction is violated.

Up to this point, collisions have been neglected under the assumption $|\omega| \gg \nu_c$. Collisional corrections to $\tilde{J}_{ze}$ in (45) and subsequently (51) of order ν_c/ω are easily obtained. These corrections, however, do not contribute to the discontinuity in $\partial\tilde{A}_z/\partial x$ once (51) is integrated.

To first order in ν_c/ω, the collisionless results in (52) are therefore still valid. The temperature gradient instability of Ref. 9 does not exist in the collisionless regime.

V. SEMI-COLLISIONAL AND COLLISIONAL TEARING INSTABILITIES

In the semi-collisional and collisional tearing instability, $\nu_c \gg |\omega|$. Over a time ω^{-1} the velocity $\mathbf{v}$ of an electron is randomized over a constant energy shell as a result of scattering with ions. The first-order distribution $\tilde{f}_e$ should therefore be a weak function of the angle variable $\xi = v_\parallel/v$. Since the Legendre polynomials $P_n(\xi)$ are eigenfunctions of the collision operator on the left side of (41), i.e.,

$$(\partial/\partial\xi)(1-\xi^2)(\partial/\partial\xi)P_n(\xi) = -n(n+1)P_n(\xi) ,$$

we expand $\tilde{f}_e$ in a Legendre series as follows:

$$\tilde{f}_e = \sum_n h_n(v)P_n(\xi) . \tag{54}$$

The right side of (41) is represented by

$$g = g_0 + g_1 P_1(\xi) , \tag{55a}$$

where

$$g_0 = e\tilde{\phi} i k_y \partial f_{0e}/\partial P_y ; \tag{55b}$$

$$g_1 = -e\tilde{E}_\parallel v \partial f_{0e}/\partial H - (e\tilde{A}_z v/c) i k_y \partial f_{0e}/\partial P_y . \tag{55c}$$

Inserting (54) and (51a) into (41), equating coefficients of $P_n(\xi)$ and retaining only h_0 and h_1, we find the coupled equations

$$i\omega h_0 - ik_\parallel v h_1/3 = g_0 ; \tag{56a}$$

$$(i\omega - \nu)h_1 - ik_\parallel v h_0 = g_1 . \tag{56b}$$

Neglecting the h_n's with $n > 1$ is justified when

$$|k_\parallel v/(i\omega - \nu)| \ll 1 . \tag{56c}$$

The present expansion is also accurate for $|\omega| \gg \nu_c$ as long as (56c) is satisfied. Equations (55) and (56) yield the solutions

$$h_1 = -iev E_\parallel(\omega\partial f_{0e}/\partial H + k_y \partial f_{0e}/\partial P_y)[(i\omega - \nu)(i\omega - k_\parallel^2 D)]^{-1} , \tag{57a}$$

$$h_0 = (k_\parallel v/3\omega)h_1 + e\tilde{\phi}k_y(\partial f_{0e}/\partial P_y)/\omega , \tag{57b}$$

where

$$D = v^2/3\nu(v) \tag{57c}$$

is the parallel electron diffusion coefficient. The perturbed electron current is then given by

$$\tilde{J}_{ze} \simeq -en_{0e}\int d\mathbf{v}\, v\xi^2 h_1 = -(2i/3\pi^{3/2})\omega_{pe}^2 \tilde{E}_\parallel \int_0^\infty dv\, v^4 v_e^{-5} \times \exp(-v^2/v_e^2)[\omega - \omega_n^* - \omega_T^*(v^2/v_e^2 - 3/2)]/[(i\omega - \nu)(i\omega - k_\parallel^2 D)] \tag{58}$$

and the electron density perturbation by

$$\tilde{n}_e = n_0 \int d\mathbf{v}\, h_0 = -k_\parallel \tilde{J}_{ze}/\omega e + k_{De}^2 \omega_{ne}^* \tilde{\phi}/4\pi\omega e . \tag{59}$$

Note that $\nu(v)$ and $D = v^2/3\nu$ are functions of v so they must be included within the integral in (58).

The ion response to $\tilde{\phi}$ depends strongly on Δ/ρ_i. We first consider the semi-collisional case where $\Delta/\rho_i \ll 1$.

A. Semi-collisional instability

When $\Delta/\rho_i \ll 1$, the ions respond to $\tilde{\phi}$ statically as in the collisionless tearing mode. Equating $\tilde{n}_e$ in (59) with $\tilde{n}_i$ in (49), one obtains an equation for $\tilde{\phi}$ analagous to (50). However, as in the collisionless case, the Doppler frequency resulting from the parallel electron motion strongly reduces $\tilde{J}_{ze}$ before $\tilde{\phi}$ is important and thus, $\tilde{\phi}$ can be neglected in (58). $\tilde{J}_{ze}$ in (58) is clearly small when $k_\parallel^2 D \gg |\omega|$. Combining (37) and (58),

$$\partial^2\tilde{A}_z/\partial x^2 = (8k_0^2\omega\tilde{A}_z/3\pi^{1/2})\int_0^\infty dv\, v^4 v_e^{-5}\nu^{-1}(i\omega - k_\parallel^2 D)^{-1} \times (1 + i\omega/\nu)\exp(-v^2/v_e^2)[\omega - \omega_n^* - \omega_T^*(v^2/v_e^2 - 3/2)] . \tag{60}$$

In (60) we have been forced to assume $|\omega| \ll \nu$ in order that the inequality in (56c) be satisfied when $k_\parallel^2 D > |\omega|$. Note, however, that corrections of order ω/ν have been retained. After integrating across the current layer to obtain the discontinuity in $\partial\tilde{A}_z/\partial z$, the v integral can be carried out. The following dispersion relation then results:

$$\omega^{1/2}\{\omega - \omega_2^* + i(\omega/\nu_c)[4\Gamma(17/4)/3\pi^{1/2}\Gamma(11/4)](\omega - \omega_2^* - 3\omega_T^*/2)\} = -\gamma_k\nu_c^{1/2}[3\pi^{1/4}/4\Gamma(11/4)]\exp(-i\pi/4);$$

$$\omega_2^* = \omega_n^* + 5\omega_T^*/4 . \tag{61}$$

The discontinuity Δ' is contained within the collisionless growth rate γ_k, and

$$\nu_c = \tau^{-1} = 16\pi^{1/2}Z^2e^4 n_{0i}\ln\Lambda/3m^2v_e^3 , \tag{62}$$

where τ is the electron-ion collision time of Braginskii.[17] The width of the current layer is defined by $k_\parallel^2 D(v) \simeq |\omega|$. Choosing $v \simeq 3v_e/2$ where the velocity integral in (60) peaks,

$$\Delta \approx \Delta_k(|\omega|\nu_c)^{1/2}/\gamma_k . \tag{63}$$

Equation (61) can easily be solved in the two regions where $\omega_2^* \gtrless \gamma_k^{2/3}\nu_c^{1/3}$. (i) When $\omega_2^* \ll \gamma_k^{2/3}\nu_c^{1/3}$, the diamagnetic drifts can be neglected and the growth rate of the tearing mode is

$$\gamma = [3\pi^{1/4}/4\Gamma(11/4)]^{2/3}\gamma_k^{2/3}\nu_c^{1/3} . \tag{64a}$$

Equation (63) for Δ then essentially reproduces (22). The assumption of unmagnetized ions requires $\Delta < \rho_i$ while our collisional approximation is valid for $|\omega| < \nu_c$, so γ in (64) is only correct when

$$1 \ll \nu_c/\gamma_k \ll (\rho_i/\Delta_k)^{3/2} . \tag{64b}$$

(ii) In the limit $\omega_2^* \gg \gamma_k^{2/3}\nu_c^{1/3}$, $\mathrm{Re}\,\omega \simeq \omega_2^*$ and growth rate of the drift tearing mode is

$$\gamma = [3\pi^{1/4}/4\Gamma(11/4)\,2^{1/2}]\gamma_k\nu_c^{1/2}/\omega_2^{*1/2} + [2\Gamma(17/4)/\pi^{1/2}\Gamma(11/4)](\omega_2^*/\nu_c)\omega_T^* . \tag{65a}$$

The first term on the right side of (65a) simply represents a reduction of the growth rate of the pure tearing mode [in (64a)] resulting from the diamagnetic drifts. The second term is driven by the temperature gradient and represents an extension of the corresponding temperature gradient driven instability of Ref. 9 to be semi-

collisional regime. From (63) the width of the current layer is

$$\Delta \simeq \Delta_k(\omega_2^* \nu_c)^{1/2}/\gamma_k \ . \tag{65b}$$

As in the collisionless case, the diamagnetic drifts broaden the region of particle acceleration. Our previous assumptions require that ω_2^* satisfy the inequality

$$(\gamma_k/\nu_c)^{2/3} \ll \omega_2^*/\nu_c \ll 1 \ , \tag{65c}$$

in addition, $\Delta \ll \rho_i$. However, it is shown in the collisional section that the results in (65) are correct even when $\Delta > \rho_i$.

The approximation that $\tilde{A}_z \simeq$ const within the region of particle acceleration again requires that the integrated phase across the layer be small. Within the limits imposed by (66) or (65c) and the restriction Δ, $\rho_i \ll a$, it is easily shown that this approximation is valid.

B. Collisional tearing instability

When $\Delta \gg \rho_i$, the ions must be considered magnetized. The parallel ion response to $\tilde{E}_\parallel$ is much weaker than that of the electrons and can be neglected. The ion density perturbation then arises from the polarization drift along the x direction [see (25)], the $\tilde{E}_y/B_z$ drift in the x direction and the finite Larmor radius correction to this drift. The following result for the ion density perturbation is well known[8]

$$\tilde{n}_i = [(c^2/c_A^2)\partial^2/\partial x^2 + k_{Di}^2(\omega_i^*/\omega)(1+\rho_i^2\partial^2/\partial x^2)]\,\tilde{\phi}/4\pi Ze \ , \tag{66}$$

where

$$\omega_i^* = -k_y U_{yi}' \ . \tag{67}$$

Since typically $c^2/c_A^2 \gg 1$, charge neutrality can again be assumed. Equating (59) and (66) and noting that charge neutrality in equilibrium requires $k_{Di}^2\omega_i^* = k_{De}^2\omega_n^*$, we find

$$(c^2/c_A^2)(\omega+\omega_i^*)\partial^2\tilde{\phi}/\partial x^2 = -4\pi k_\parallel \tilde{J}_{ze} \ , \tag{68}$$

where $\tilde{J}_{ze}$ is given by (58). In the collisional tearing mode $\tilde{E}_\parallel \to 0$ before $k_\parallel^2 D \sim |\omega|$ so Eq. (58) for $\tilde{J}_{ze}$ simplifies to

$$\tilde{J}_{ze} = \sigma(\omega)\tilde{E}_\parallel \ , \tag{69}$$

where

$$\sigma(\omega) = -(2/3\pi^{3/2})\,\omega_{pe}^2 \int_0^\infty ds\, s^4 \frac{\exp(-s^2)}{i\omega - \nu(sv_e)} \times [\omega - \omega_n^* - \omega_T^*(s^2-3/2)]/\omega \tag{70}$$

is the generalized conductivity of a Lorentz gas. When $\omega \ll \nu_c$,

$$\sigma(\omega) \simeq \sigma_L[\omega - \omega_n^* - 5\omega_T^*/2 + i(105/16)(\omega/\nu_c) \times (\omega - \omega_n^* - 4\omega_T^*)]/\omega \ , \tag{71a}$$

where

$$\sigma_L = 2(2T_e)^{3/2}/\pi^{3/2} m^{1/2} e^2 \ln\Lambda \tag{71b}$$

is the classical conductivity of a Lorentz gas.[5] In the regime where $\omega \gg \nu_c$,

$$\sigma(\omega) = i(\omega_{pe}^2/4\pi\omega^2)[\omega - \omega_n^* - \omega_T^* - i(\nu_c/\omega)(\omega - \omega_n^* + \omega_T^*/2)] \tag{72}$$

Equations (37), (68), and (69) yield the following coupled equations for $\tilde{\phi}$ and $\tilde{A}_z$:

$$\partial^2\tilde{A}_z/\partial x^2 = -i(4\pi/c)\sigma(\omega\tilde{A}_z/c - k_\parallel\tilde{\phi}) \ ; \tag{73}$$

$$[(\omega+\omega_i^*)(c^2/c_A^2)\partial^2/\partial x^2 - i4\pi k_\parallel^2\sigma]\,\tilde{\phi} = -i4\pi k_\parallel \omega\sigma\tilde{A}_z/c \ , \tag{74}$$

where we have expressed $E_\parallel$ in terms of $\tilde{\phi}$ and $\tilde{A}_z$. As discussed previously in Sec. II, when the second term on the left side of (74) becomes large compared with the first term, $\tilde{E}_\parallel \to 0$ and the right side of (73) becomes small. To show this, we again assume $\tilde{A}_z \simeq$ const within the narrow current layer and rewrite (73) and (74) as

$$\partial^2\tilde{A}_z/\partial x^2 \simeq -(4\pi i\omega\sigma/c^2)\tilde{A}_z(0)(1-xy) \ ; \tag{75}$$

$$(\partial^2/\partial x^2 - x^2/\delta^4)\,y = -x/\delta^4 \ , \tag{76}$$

where

$$y = k_y c\tilde{\phi}/\tilde{A}_z(0)\omega l_s \ ; \tag{77}$$

$$\delta^4 = -i(\omega+\omega_i^*)c^2 l_s^2/k_y^2 4\pi\sigma c_A^2 \ . \tag{78}$$

We want the solution to (76) which varies asymptotically as $y \sim x^{-1}$. Equation (76) can be solved by defining a new dependence variable y/x and a new independent variable x^2 and then Fourier transforming the resulting equation. The solution, which has been obtained previously, is[19]

$$y = (x/2\delta^2)\int_0^{\pi/2} d\theta \sin^{1/2}\theta \exp(-x^2\cos\theta/2\delta^2) \ . \tag{79}$$

This solution goes asymptotically to $y \sim x^{-1}$ when $\mathrm{Re}(x^2/2\delta^2) \gtrsim 1$ so the width of the current layer is roughly

$$\Delta \simeq [2/\mathrm{Re}(\delta^{-2})]^{1/2} \ . \tag{80}$$

It is evident from (79) and (80) that the solution in (79) has the correct asymptotic dependence only when

$$\mathrm{Re}(\delta^2) > 0 \ . \tag{81}$$

The mismatch Δ' is then obtained by inserting the solution for y into (75) and integrating the resultant equation. The dispersion relation is

$$\omega\sigma(\omega)\delta(\omega) = ic^2\Gamma(1/4)\Delta'/8\pi^2\Gamma(3/4) \ , \tag{82}$$

which can be rewritten, using (78) as

$$\omega^4(\omega+\omega_i^*)\sigma^3(\omega) = 4\pi i(k_y c_A/cl_s)^2[c^2\Gamma(1/4)\Delta'/8\pi^2\Gamma(3/4)]^4 \tag{83}$$

Care must be taken that no extraneous roots were introduced in going from (82) to (83). The dispersion relation in (83) can be solved analytically in the two limits where $\omega \gtrless \nu_c$.

(i) When $\omega \ll \nu_c$, $\sigma(\omega)$ is given by (71) and (83) can be expressed as

$$\omega(\omega+\omega_i^*)[\omega - \omega_3^* + i(105/16)(\omega/\nu_c)(\omega - \omega_3^* - 3\omega_T^*/2)]^3 = i\gamma_c^5 \ , \tag{84a}$$

where

$$\omega_3^* = \omega_n^* + 5\omega_T^*/2 \tag{84b}$$

and

$$\gamma_c = [\Gamma(1/4)/2\pi\Gamma(3/4)]^{4/5}(k_y a^2/l_s)^{2/5}(\Delta' a)^{4/5}\tau_A^{-2/5}\tau_s^{-3/5} \tag{84c}$$

is the classical growth rate of the collisional tearing mode[4] expressed in terms of the Alfvén time $\tau_A = a/c_A$ and the resistive skin time $\tau_s = 4\pi a^2\sigma_L/c^2$ of the plasma.

In terms of the collisionless growth rate γ_k and layer thickness Δ_k,

$$\gamma_c = \nu_c^{3/5}\gamma_k^{2/5}(\Delta_k/\rho_i)^{2/5}(27\pi T_i/ZT_e)^{1/5}[\Gamma(1/4)/\Gamma(3/4)]^{4/5}/8 \ . \tag{84d}$$

(a) For $\gamma_c \gg \omega_3^*$, the gradient drifts can be neglected and we recover the usual collisional result,[4]

$$\omega = i\gamma_c \ . \tag{85}$$

The width of the current layer calculated from (80) essentially reproduces (30) while the conditions that $\Delta_c \gg \rho_i$ and $k_\parallel^2 D \ll \gamma_c$ yield (31). The constant $\tilde{A}_z$ approximation requires

$$k_0^2\gamma_c\Delta_c^2/\nu_c = (\Delta' a)(\Delta_c/a) \ll 1, \tag{86}$$

which is easily satisfied if $\Delta_c/a \ll 1$.

(b) When $\gamma_c \ll \omega_3^*$, Re $\omega \simeq \omega_3^*$ and

$$\omega \simeq \omega_3^* + i(315/32)(\omega_3^*/\nu_c)\,\omega_T^* + i^{1/3}[\gamma_c^5/(\omega_3^* + \omega_i^*)\,\omega_3^*]^{1/3} \ . \tag{87}$$

Barring numerical factors the third term on the right side of (87) is the same as that found by Coppi[8] and the second term represents the temperature gradient instability of Ref. 9. The layer width, as calculated from (80), is

$$\Delta \simeq (\omega_3^*/\gamma_c)^{2/3}\Delta_c \ . \tag{88}$$

As in the collisional and semi-collision regimes, the gradient drifts broaden the region of particle acceleration.[8] If ω^* becomes too large (or ν_c too small), we therefore expect the electron Doppler frequency rather than electrostatic effects to limit the width of the layer. The semi-collisional results in (65a) are then valid. In the collisional regime the inequality $\omega^* \gg k_\parallel^2 D = k_y^2(\omega^*/\gamma_c)^{4/3}\Delta_c^2 D/l_s^2$ must be satisfied, or for $v \simeq 2v_e$

$$\nu_c \gg (\rho_i/\Delta_k)^{4/3}\gamma_k^{2/3}\omega^{*1/3} \ . \tag{89}$$

A simple calculation shows that the growth rates in (65a) and (87) roughly match at the boundary where the left and right sides of (89) are comparable. Our previous assumptions also require $\nu_c \gg \omega^* \gg \gamma_c$.

(ii) When $\omega \gg \nu_c$, $\sigma(\omega)$ is given by (72) and the dispersion relation in (83) takes the form

$$[\omega - \omega_4^* - i(\nu_c/\omega)(\omega - \omega_4^* + 3\omega_T^*/2)]^3(\omega + \omega_i^*)/\omega^2 = -\Gamma_k^2 \ , \tag{90a}$$

where

$$\omega_4^* = \omega_n^* + \omega_T^* \tag{90b}$$

and

$$\Gamma_k = (T_i/ZT_e)^{1/2}(\Delta_k/\rho_i)\gamma_k[\Gamma(1/4)/\Gamma(3/4)]^2/\pi \tag{90c}$$

is the growth rate of the previous collisionless tearing mode.[7]

(a) When $\omega_4^* \ll \Gamma_k$, the gradient drifts can be neglected and $\omega = i\Gamma_k$. However, in the limit $\omega \gg \nu_c$, the plasma is essentially collisionless so it is not surprising that the width of the current channel as calculated from (80) yields the previous collisionless result in (53b), which is much *smaller* than an ion Larmor radius. Hence, the result $\omega = i\Gamma_k$ for the collisionless tearing mode is inconsistent since we have assumed $\Delta \gg \rho_i$.

(b) In the opposite limit where $\omega_4^* \gg \Gamma_k$, we will now demonstrate that there is also no self-consistent solution to (90a). In the collisionless calculation in Sec. IV, it was found that $\Delta \propto \omega^*$ when $\omega^* \gg \gamma_k$, Δ being given by the condition $\omega^* \simeq k_\parallel v_e$. For sufficiently, large ω^*, we then expect $\tilde{E}_\parallel \to 0$ before $k_\parallel v_e \simeq \omega^*$, i.e., the dispersion relation in (90a) is then valid. Solving (90a) when $\omega^* \gg \Gamma_k$ and calculating Δ from (80), we indeed find that $k_\parallel v_e \ll \omega^*$ as long as

$$\omega^* \gg \gamma_k(\rho_i/\Delta_k)^2 \ . \tag{91}$$

Unfortunately, the layer is so broad for such large values of ω^* that the constant $\tilde{A}_z$ approximation is grossly violated. A more refined description of the coupling between $\tilde{A}_z$ and $\tilde{\phi}$ is then needed to describe the high limit.

The collisionless theory in Sec. IV is evidently limited by the constant $\tilde{A}_z$ assertion rather than by the neglect of electrostatic effects. The inequality in (53), therefore defines the maximum ω^* for which the theory is valid, i.e.,

$$\omega^* \ll \gamma_k/(k_0\Delta_k)^2 \ . \tag{92}$$

VI. SUMMARY AND DISCUSSION

The interesting physics of the tearing instability is associated with the narrow layer around $\mathbf{k}\cdot\mathbf{B} = 0$ where a parallel electric field accelerates the electrons along $\mathbf{B}_0$. The dynamics of this layer depends strongly on the electron-ion collision frequency ν_c. In particular, the tearing mode separates into three regimes which we refer to as collisionless, semi-collisional, and collisional. In the collisionless and semi-collisional regimes the region of particle acceleration ("singular layer") is limited by the electron thermal motion along B_0, the width Δ of the layer being determined by the condition $\omega_D = |\omega|$, where ω_D is the effective Doppler frequency of the electrons and ω is the complex wave frequency. In the collisional regime Δ is determined by the condition $\tilde{E}_\parallel = -ik_\parallel\tilde{\phi} + i\omega\tilde{A}_\parallel/c = 0$, where the parallel component of the induced electric field is balanced by the parallel electrostatic field. Simple physical descriptions of the tearing mode in the three regimes are presented in Sec. II.

The effect of both density and temperature gradients have been investigated. Within each of the three regions of collisionality, the purely growing tearing mode transforms into the oscillatory, drift-tearing mode as the diamagnetic frequency ω^* (evaluated at $\mathbf{k}\cdot\mathbf{B} = 0$) increases. The drift-tearing mode is characterized by having Re $\omega \simeq \omega^*$.

Our results for the pure tearing instability ($\omega^* \simeq 0$) are summarized in Table I where the analytic expressions for the growth rates γ and layer widths Δ in the three regimes are displayed. γ and Δ are plotted against $\nu_c(\nu_c = \tau^{-1}$, where τ is the electron-ion collision time of Braginskii[17]) in Figs. 5 and 6, respectively. γ has been normalized to the collisionless growth rate γ_k[15], which differs from the previously accepted expression[7,9] which has been found to be incorrect. Δ has been normalized to the collisionless layer width $\Delta_k \simeq (k_0^2 a)^{-1}$, where k_0^{-1} is the collisionless skin depth. Typically, $\Delta_k \ll k_0^{-1}$, ρ_i.

TABLE II. Drift-tearing instability.

	Frequency/growth rate	Width layer	Restrictions
IV Collisionless	$\omega_1^* = \omega_n^* + \omega_T^*/2$ $\gamma_k = \dfrac{k_y v_e (\Delta' a)}{2\pi^{1/2} k_0^2 a l_s}$	$\Delta \simeq \left(1 + \dfrac{\omega^{*2}}{\gamma_k^2}\right)^{1/2} \Delta_k$	$\nu_c \ll \omega^*$ $\omega^* \gg \gamma_k$
V Semi-collisional	$\omega_2^* = \omega_n^* + 5\omega_T^*/4$ $\gamma = \left[\dfrac{3\pi^{1/4}}{2^{1/2} 4\Gamma(11/4)}\right] \dfrac{\gamma_k \nu_c^{1/2}}{\omega_2^{*1/2}}$ $+ \left[\dfrac{2\Gamma(17/4)}{\pi^{1/2}\Gamma(11/4)}\right] \dfrac{\omega_2^*}{\nu_c} \omega_T^*$	$\Delta \simeq \Delta_k \dfrac{(\omega^* \nu_c)^{1/2}}{\gamma_k}$	$\omega^{*1/3} \gamma_k^{2/3} (\rho_i/\Delta_k)^{4/3} \gg \nu_c \gg \omega^*$ $\omega^* \gg (\nu_c \gamma_k^2)^{1/3}$
VI collisional	$\omega_3^* = \omega_n^* + 5\omega_T^*/2$ $\gamma = \left(\dfrac{315}{32}\right) \dfrac{\omega_3^*}{\nu_c} \omega_T^*$ $+ \left[\dfrac{\gamma_c^5}{\omega_3^*(\omega_3^* + \omega_i^*)}\right]^{1/3} \mathrm{Im}(i^{1/3})$	$\Delta \simeq (\omega^*/\gamma_c)^{2/3} \Delta_c$ $\simeq (\omega^*/\gamma_k)^{2/3} \rho_i^{2/3} \Delta_k^{1/3}$	$\nu_c \gg \omega^{*1/3} \gamma_k^{2/3} (\rho_i/\Delta_k)^{4/3}$ $\omega^* \gg \gamma_k^{2/5} \nu_c^{3/5} (\Delta_k/\rho_i)^{2/5}$

Note that the transition from the semi-collisional to the collisional tearing-mode occurs at $\nu_c/\gamma_k \simeq (\rho_i/\Delta_k)^{3/2}$, where $\Delta \simeq \rho_i$.

The results of our investigation of the drift-tearing instability are summarized in Table II where analytic expressions for γ and Δ are presented. The range of ν_c defining the three regimes of the instability is presented. In addition, the requirement on ω^* for the instability to be of the "drift-tearing" type is indicated. In all cases, the diamagnetic drift serves to broaden Δ. The physical explanation of this result has been presented in Sec. III. γ is unaffected by ω^* in the collisionless regime while in the semi-collisional and collisional regimes it is strongly modified. In the absence of the temperature gradient, as represented by ω_T^* [see (46b) and 33d)], a comparison of Tables I and II shows that in the semi-collisional and collisional regimes, ω^* reduces γ. However, an additional destabilizing turn proportional to ω_T^* may be quite large. This temperature gradient instability has been previously investigated by Hazeltine *et al.*,[9] whose calculations have been found to be valid only in the collisional regime. The growth rate which we obtain in the collisional regime differs in numerical factors from that found in Refs. 8 and 9 because of our neglect of electron-electron collisions.

The region of validity of the various instabilities presented in Tables I and II can easily be visualized in the $\omega^* - \nu_c$ phase space shown in Fig. 7. The vertical axis is $\omega^*/\gamma_k = p$ with the horizontal axis $\nu_c/\gamma_k = q$. The semi-collisional regime has been shaded, the collisonless regime lying to the left and the collisional regime to the right. The dashed line designates the boundary between the tearing and drift-tearing instabilities. The six regimes of the tearing mode are represented by the Roman numerals I through VI, the appropriate expressions for γ and Δ in each region being labeled by the same numeral in Tables I and II. The only variable in the phase space of Fig. 7 is the position of the right hand boundary of the semi-collisional regime, which is given by $q = \nu_c/\nu_k = R^{3/2}$, where $R = \rho_i/\Delta_k \gg 1$. The slopes of all the boundaries are universal.

To determine which of the six regimes shown in Fig. 7 is relevant to a particular experiment, one merely calculates the collisionless growth rate γ_k and layer width Δ_k (defined in Table I), the ion Larmor radius ρ_i, ω^* and ν_c for the particular mode of interest. Figure 7 can then be used to determine which of the six regions is appropriate and the growth can be found in Tables I or II.

We now investigate the relevance of our calculations to some typical tokamak discharges. We specifically consider a cylindrical model of the tokamak where toroidal effects are neglected. This approximation is very good in high aspect ratio machines such as the ST but is

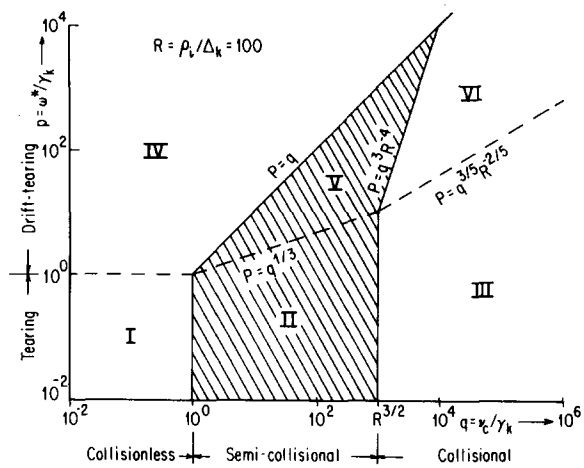

FIG. 7. The regions of validity of the "collisionless", "semi-collisional" and "collisional" regimes are shown in the $\omega^* - \nu_c$ phase space. ω^* is represented by the normalized quantity $p \simeq \omega^*/\gamma_k$ and ν_c by $q = \nu_c/\gamma_k$, γ_k being the collisionless growth rate. The dashed line indicates the boundary between the tearing and drift tearing instabilities. The tearing mode evidently separates into six regions represented by the Roman numerals I through VI. The growth rates γ and layer widths Δ are listed in Tables I and II under the corresponding numerals. After calculating q, p and $R = \rho_i/\Delta_k$ for the rational surface of interest in a particular tokamak discharge, the appropriate region of interest can be readily determined from Fig. 7.

TABLE III. Typical discharge parameters and $m=2$ mode characteristics.

	ALCATOR	PLT
a (cm)	9.5	45
R(cm)	54	130
B_T(kG)	50	45
Z_{eff}	1	3
n_e(cm^{-3})	5×10^{13}	7×10^{13}
T_e(keV)	1	2
ρ_i(cm)	0.063	0.1
ν_c(kHz)	210	280
m,n	2, 1	2, 1
r_s(cm)	$a/2$	$a/2$
ω^*(kHz)	~ 84	~ 8.7
$\Delta' a$	~ 4	~ 4
Δ_k(cm)	5.6×10^{-4}	0.89×10^{-4}
$R=\rho_i/\Delta_k$	110	1100
γ_k(kHz)	2.8	0.06
$\left[\frac{\omega^*\gamma_k^2}{\nu_c^3}\left(\frac{\rho_i}{\Delta_k}\right)^4\right]^{1/3}$	22 (semi-collisional)	13 (semi-collisional)
$\omega^*/\gamma_k^{2/3}\nu_c^{1/3}$	9.1 (drift-tearing)	8.9 (drift-tearing)
Δ(cm)	0.027	0.073
γ(kHz)	97	0.9
T_{c-sc}(eV)	330	800

questionable in devices of lower aspect ratio such as PLT or Microtor. The inclusion of toroidal effects, however, is beyond the scope of this paper.

In cylindrical geometry the equilibrium magnetic field of a tokamak contains both axial and azimuthal components, represented by $B_{0z}(r)$ and $B_{0\theta}(r)$, respectively. A perturbation periodic over a length $2\pi R$, R being the major radius of the torus, then has a wavevector $\mathbf{k}=(m/r)\hat{e}_\theta+(n/R)\hat{e}_z$ and typically $k\simeq m/r$. The regions of particle acceleration (near $\mathbf{k}\cdot\mathbf{B}=0$) then occur at discrete radii r_s where $q=r_sB_{0z}(r_s)/RB_\theta(r_s)=m/n$, q being the safety factor. To extend our results to cylindrical geometry, one makes the following replacements:

$$k_y \to m/r_s\ ;$$

$$l_s \to (R/r_s)(m/n)\left|d\ln q/dr_s\right|^{-1} \tag{93}$$

l_s being the magnetic shear length [see Eq. (6)]. Δ' has been calculated in cylindrical geometry for various current profiles in Ref. 10.

We now consider the relevance of these calculations to some typical tokamak discharges. Alcator and PLT are selected as examples. Typical operating parameters for these machines are displayed in Table III along with the characteristics of an $m=2$, $n=1$ tearing mode which is assumed to have a rational surface at $r_s\simeq a/2$. The collisionless tearing widths Δ_k of both machines are much smaller than an ion Larmor radius, Δ_k being an order of magnitude smaller in PLT than in Alcator. The collisionless growth rate γ_k is also smaller in PLT. The lower value of γ_k in PLT is a consequence of the large minor radius a of this machine. The magnetic energy density driving the tearing instability[20] is proportional to $\Delta'\simeq a^{-1}$, while the wavelength of the $m=2$ mode scales like "a". Both of these effects tend to reduce γ_k in PLT. γ_k and Δ_k are, of course, not physical quantities since neither of the two machines are in the collisionless regime.

For the parameters displayed in Table III the $m=2$ mode in both machines falls in the semi-collisional, drift-tearing region (area V in Fig. 7). The growth rates γ and "singular layer" widths Δ have been calculated from Table II. The instability in both machines is driven primarily by the temperature gradient (represented by ω_T^* in Table III). γ is two orders of magnitude smaller in PLT than in Alcator because its large minor radius effectively increases the scale length of the temperature gradient and thus reduces the driving force of the instability. Δ is somewhat smaller than ρ_i in both machines. It should be emphasized, however, that in the semi-collisional regime, the tearing instability is virtually independent of the ion dynamics and therefore, the theory is valid even if $\Delta\simeq\rho_i$.

The boundary between the semi-collisional and collisional regimes of the drift-tearing mode (see Fig. 7) is very sensitive to T_e since $(PR^4)^{1/3}/q\propto T_e^3$. For low temperature discharges in Alcator and PLT, the $m=2$ mode consequently falls in the collisional regime. For the parameters in Table III the transition from the semi-collisional to the collisional regimes occurs at 300 and 800 eV in Alcator and PLT, respectively.

Calculations similar to those presented for Alcator and PLT have been carried out for the ST, Microtor, ORMAK, and Macrotor. The characteristics of the $m=2$ tearing mode in the first three machines are similar to those in Alcator while the $m=2$ mode in Macrotor closely resembles that in PLT.

ACKNOWLEDGMENTS

We would like to acknowledge Professor F. V. Coroniti for stimulating our interest in tearing instabilities and for participating in many helpful conversations, and J. M. Van Dam for carefully reading the manuscript.

This work was supported in part by the Energy Research and Development Administration, Contract No. E(11-1)-GEN 10, P.A. 26, and the National Science Foundation Contract No. PHY 75-07809 A01.

[1] J. C. Hosea, C. Bobeldijk, and D. J. Grove, in *Plasma Physics and Controlled Nuclear Fusion Research* (International Atomic Energy Agency, Vienna, 1971), Vol. II, p. 425.

[2] S. V. Mirnov and I. B. Semenov, in *Plasma Physics and Controlled Nuclear Fusion Research* (International Atomic Energy Agency, Vienna, 1971), Vol. II, p. 401; S. V. Mirnov and I. B. Semenov, Zh. Eksp. Teor. Fiz. 60, 2105 (1971) [Sov. Phys.-JETP 33, 1134 (1971)].

[3] J. W. Dungey, *Cosmic Electrodynamics* (Cambridge Univer-

sity, Cambridge, 1958), p. 98.
[4]H. P. Furth, J. Killeen, and M. N. Rosenbluth, Phys. Fluids 6, 459 (1963).
[5]L. Spitzer, *Physics of Fully Ionized Gases* (Wiley, New York, 1962), p. 136.
[6]H. P. Furth, Nucl. Fusion Suppl. Pt. 1, 169 (1961).
[7]B. Coppi, Phys. Fluids 8, 2273 (1965).
[8]B. Coppi, Phys. Fluids 7, 1501 (1964).
[9]R. D. Hazeltine, D. Dobrott, and T. S. Wang, Phys. Fluids 18, 1778 (1975).
[10]H. P. Furth, P. H. Rutherford, and H. Selberg, Phys. Fluids 16, 1054 (1973).
[11]J. M. Finn, Bull. Am. Phys. Soc. 20, 1219 (1975); A. B. Rechester and T. H. Stix, Phys. Rev. Lett. 36, 587 (1976).
[12]R. D. Hazeltine and H. R. Strauss, Phys. Rev. Lett. 37, 102 (1976).
[13]O. Kluber, F. Karger, and G. Fussmann, Bull. Am. Phys. Soc. 21, 1050 (1976).
[14]P. H. Rutherford, Phys. Fluids 16, 1903 (1973); B. V. Waddell, M. N. Rosenbluth, D. A. Monticello, and R. B. White, Bull. Am. Phys. Soc. 20, 1342 (1975).
[15]G. Laval, R. Pellat, and M. Vuillemin, in *Plasma Physics and Controlled Nuclear Fusion Research* (International Atomic Energy Agency, Vienna, 1965), Vol. II, p. 259.
[16]It has come to our attention that C. S. Liu and M. N. Rosenbluth have obtained a similar result (private communication).
[17]S. I. Braginskii, in *Reviews of Plasma Physics*, edited by M. A. Leontovich (Consultants Bureau, New York, 1965), Vol. I, p. 205.
[18]R. D. Fried and S. D. Conte, *The Plasma Dispersion Function* (Academic, New York, 1961).
[19]P. H. Rutherford and H. P. Furth, Princeton Plasma Physics Laboratory Report Matt-872 (1971).
[20]H. P. Furth, in *Propagations and Instabilities in Plasmas*, edited by W. I. Futterman (Stanford University, Stanford, Calif., 1963), p. 87.